

Field emission of carbon nanotubes on anodic aluminum oxide template with controlled tube density

Po-Lin Chen, Jun-Kai Chang, Cheng-Tzu Kuo, and Fu-Ming Pan

Citation: [Applied Physics Letters](#) **86**, 123111 (2005); doi: 10.1063/1.1886260

View online: <http://dx.doi.org/10.1063/1.1886260>

View Table of Contents: <http://scitation.aip.org/content/aip/journal/apl/86/12?ver=pdfcov>

Published by the [AIP Publishing](#)

Articles you may be interested in

[Carbon nanotubes synthesized by biased thermal chemical vapor deposition as an electron source in an x-ray tube](#)

Appl. Phys. Lett. **86**, 123115 (2005); 10.1063/1.1891299

[Vertically aligned carbon nanofibers and related structures: Controlled synthesis and directed assembly](#)

J. Appl. Phys. **97**, 041301 (2005); 10.1063/1.1857591

[Growth of multiwalled-carbon nanotubes using vertically aligned carbon nanofibers as templates/scaffolds and improved field-emission properties](#)

Appl. Phys. Lett. **86**, 053110 (2005); 10.1063/1.1852730

[Growth behavior and interfacial reaction between carbon nanotubes and Si substrate](#)

J. Vac. Sci. Technol. A **22**, 1461 (2004); 10.1116/1.1735908

[Field emission of large-area and graphitized carbon nanotube array on anodic aluminum oxide template](#)

J. Appl. Phys. **93**, 5602 (2003); 10.1063/1.1564882

The advertisement features a dark blue background with white and orange text. At the top left, it reads 'NEW! Asylum Research MFP-3D Infinity™ AFM' in large white letters, followed by 'Unmatched Performance, Versatility and Support' in orange. To the right is the Oxford Instruments logo, which includes the text 'OXFORD INSTRUMENTS' and 'The Business of Science®'. Below the main text are four images with descriptive text: 1) A blue textured surface with the text 'Stunning high performance'. 2) A brown textured surface with the text 'Simpler than ever to GetStarted™'. 3) A yellow and brown patterned surface with the text 'Comprehensive tools for nanomechanics'. 4) A white and blue AFM instrument with the text 'Widest range of accessories for materials science and bioscience'. The instrument is shown from a three-quarter view.

Field emission of carbon nanotubes on anodic aluminum oxide template with controlled tube density

Po-Lin Chen, Jun-Kai Chang, Cheng-Tzu Kuo, and Fu-Ming Pan^{a)}

Department of Materials Science and Engineering, National Chiao Tung University, Hsinchu, Taiwan

(Received 2 November 2004; accepted 13 February 2005; published online 17 March 2005)

The tube number density of aligned carbon nanotubes (CNTs) grown over the nanoporous anodic aluminum oxide (AAO) template can be directly controlled by adjusting the CH_4/H_2 feed ratio during the CNT growth. We ascribe the variation of the tube density as a function of the CH_4/H_2 feed ratio to the kinetic competition between outgrowth of cobalt-catalyzed CNTs from the AAO pore bottom and deposition of the amorphous carbon (*a*-C) overlayer on the AAO template. A pore-filling ratio of 18% to 82% for the nanotubes overgrown out of nanopores on the AAO template can be easily achieved by adjusting the CH_4/H_2 feed ratio. Enhanced field emission properties of CNTs were obtained by lowering the tube density on AAO. However, at a high CH_4 concentration, *a*-C by-product deposit on the CNT surface can degrade the field emission property due to a high energy barrier and significant potential drop at the emission site. © 2005 American Institute of Physics. [DOI: 10.1063/1.1886260]

Carbon nanotubes (CNTs) have become one of the most promising candidates for field electron emitters to be used in future generations of cold-cathode flat panel displays and various vacuum microelectronic devices.¹ For field emission display application, it is necessary to grow vertically aligned CNT arrays on a large area with suitable tube density and tube dimensions. In recent years, template methods, such as anodic aluminum oxide (AAO) nanotemplates in particular, have been widely introduced to produce well aligned and monodispersed CNT arrays.² When CNTs are grown in the AAO template without transition metal catalyst, the diameter, the length, the arrangement, and the packing density of nanotubes can faithfully replicate the pattern of the AAO nanopore structure. However, these tubes are very poor in graphitization.³ In the case of metal catalyst assisted growth of CNTs in the AAO template, crystallinity of CNTs can be remarkably improved, but a relatively high tube growth rate will lead to overgrowth and entanglement of the dense nanotubes.⁴ Since the field emission property of CNTs is greatly affected by the field-screening effect caused by neighboring nanotubes,⁵ it is necessary to well control the length and the spacing of CNTs. In this letter, we report that the tube density of the cobalt-catalyzed CNTs on the AAO template can be controlled by regulating the flow rate ratio of methane (CH_4) to hydrogen (H_2) precursor gases during the CNT growth, and thereby field emission characteristics of CNTs can be adjusted.

In the experiment, two-step anodization, which has been reported in detail elsewhere,⁶ was used to prepared ordered AAO pore channel arrays. The Co catalyst for the CNT growth was electrochemically deposited at the pore bottom. The CNT growth was carried out in the microwave plasma (2.45 GHz) electron cyclotron resonance chemical deposition (ECR-CVD) system under a magnetic field strength of 875 Gauss. The gas mixture of CH_4 and H_2 was used as the carbon source. The total gas flow rate was kept constant at 22 sccm. The other growth conditions were: microwave

power 700 W, substrate bias -150 V, working pressure 0.25 Pa, growth temperature 600°C , and growth time 30 min. The CH_4 concentration in the gas precursor was varied from 9% to 91% in order to investigate the influence of the CH_4/H_2 ratio on the CNT growth. Figures 1(a)–1(c) show the side-view scanning electron micrographs (SEM) of the AAO templated CNTs grown at CH_4 concentrations of 9%, 50%, and 91%, respectively. As shown, the CNT density changes dramatically depending on the carbonaceous gas content. At the CH_4 concentration of 9% [see Fig. 1(a)], the tube density of CNT is as high as 9.0×10^9 tubes/ cm^2 , indicating a pore-filling ratio of about 82%, which is defined as the density ratio of the nanotubes to the AAO pores. At an extremely high CH_4 concentration of 91% [see Fig. 1(c)], the

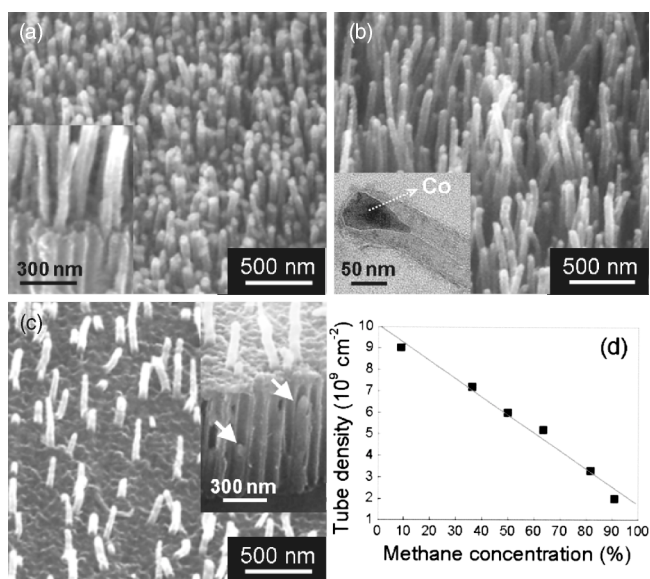


FIG. 1. Side-view SEM images of the AAO templated CNTs grown at CH_4 concentrations of (a) 9%, (b) 50%, and (c) 91%. The insets in (a) and (c) are the cross-sectional view of the CNTs. The inset in (b) is the TEM image of the CNT. (d) The tube density of CNTs grown over the AAO nanopores as a function of the CH_4 concentration.

^{a)}Electronic mail: fmpan@faculty.nctu.edu.tw

tube density decreases significantly to about 2.0×10^9 tubes/cm², corresponding to a pore-filling ratio of about 18%. The inset in Fig. 1(b) shows the transmission electron microscopy (TEM) image of the CNTs. It clearly shows that a Co catalyst particle is encapsulated at the tube tip and covered by graphitic cap, suggesting that the CNT growth is via the tip-growth mechanism.⁷

While the Co-catalyzed CNTs were grown in the AAO template, deposition of carbonaceous by-product on the AAO template took place simultaneously.⁸ As shown in Fig. 1(c), the AAO surface was covered by a thin layer of deposit, which seriously blocked the outgrowth of CNTs. Auger electron spectroscopy (AES) was used to study the chemical composition of the deposit. The shape of the carbon (KVV) peak in the Auger spectrum (not shown) reveals that the deposit is most likely composed of amorphous carbon (*a-C*). The *a-C* layer is formed by plasma decomposition of CH₄ and H₂, and deposited on the AAO surface during the CNT growth, in particular, at high CH₄/H₂ feed ratios.⁹ The *a-C* deposition seems to play an important role in control of the tube density of CNTs on the AAO template. During the CNT growth in the CH₄/H₂ plasma, the *a-C* by-product is concurrently deposited on the AAO template, whereas it can be quickly etched away by reactive hydrogen species in the plasma.¹⁰ At a high CH₄/H₂ feed ratio, the *a-C* deposition overwhelms the etch reaction, resulting in steady growth of the *a-C*.⁹ The *a-C* layer will gradually cover up the AAO nanopores and prevent nanotubes from growing out of the nanopores. As shown in the inset of Fig. 1(c), some short nanotubes marked by white arrows are buried inside the nanopores. Those CNTs which have already grown out of the nanopores can continuously grow up since the CNT growing site is at the tip of the nanotubes (tip-growth mechanism). At the CH₄ concentration of 91%, only about 18% of CNTs grew out of the AAO nanopores. On the other hand, at a low CH₄/H₂ feed ratio, the AAO surface is almost free from the *a-C* layer [see the inset of Fig. 1(a)] since it was quickly etched away by hydrogen species, leading to efficient CNT growth and thus a very high tube density. Figure 1(d) shows that the tube density is inversely proportional to the CH₄ concentration. In addition to the tube density, the CNTs grown at CH₄ concentration of 91% are shorter than those grown at 50% and 9% as shown in Figs. 1(a)–1(c). This is probably due to that the *a-C* layer may also be deposited on the CNT, which can hinder reactive carbonaceous species from reaching the Co catalyst, hence reducing the CNT growth rate.

Figure 2 shows the field emission current density (*J*) as a function of the applied electric field (*E*) for the AAO templated CNTs with three different tube densities shown in Figs. 1(a)–1(c). Measurements were conducted by the simple diode configuration and performed in a vacuum about 10⁻⁶ Torr. The anode is a platinum wire with a hemispherical tip 1 mm in diameter. The distance between the CNTs and the anode was about 100 μm. The CNT film with the highest density of 9.0×10^9 tubes/cm² shows the worst emission property in terms of the highest turn-on electric field (*E*_{to}) (8.1 V/μm) and the lowest current density, where *E*_{to} is defined herein as the electric field required to produce an emission current density of 1 mA/cm². As the tube density decreases to about 6.0×10^9 tubes/cm², the field emission property is remarkably improved (*E*_{to} ~ 5.2 V/μm). However, when the tube density decreases further to about 2.0

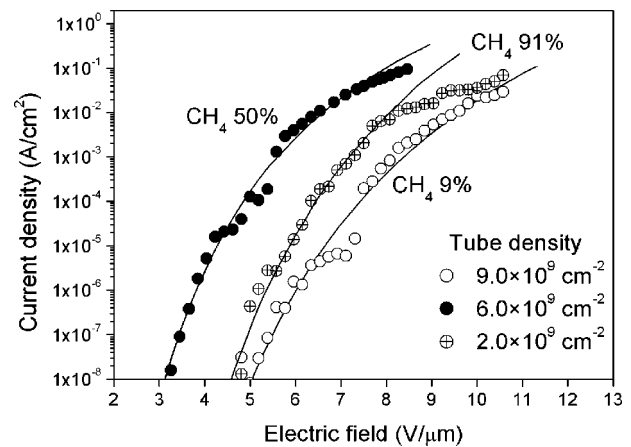


FIG. 2. Field emission current density (*J*) as a function of electric field (*E*) for the CNTs grown on the AAO template with the three different tube densities shown in Figs. 1(a)–1(c). The solid curves are F–N fits using the low current/field regions which do not show saturation.

$\times 10^9$ tubes/cm² the field emission property deteriorates (*E*_{to} ~ 7.4 V/μm). The dependence of the emission current on the applied electric field for a tip emitter can be described via the Fowler–Nordheim (F–N) relation¹¹

$$J \propto E_{\text{loc}}^2 \exp(-6.8 \times 10^7 \Phi^{3/2}/E_{\text{loc}}), \quad (1)$$

where Φ is the local work function of the emitter tip, and *E*_{loc} is the effective local electric field at the tip. According to the relation, the emission current is only dependent on the local electric field at the emission site assuming a constant work function on the emitter tip. The local field depends on the applied bias (*V*) and the radius (*R*) of a free-standing emitter tip, yielding $E_{\text{loc}} = V/kR$, where *k* is a geometric factor with a value between 1 and 5. According to the SEM micrographs shown in Fig. 1, the CNTs grown at different CH₄ concentrations show little difference in the tip radius and shape, and hence all the three CNT samples presumably have similar values of *k* and *R*. The three samples differ in morphology mainly by two parameters, the tube density, and length. The better field emission characteristic of the CNT film deposited with 50% CH₄ compared with the sample with 9% CH₄ is probably due to a slighter field-screening effect.⁵ However, it has been reported that a single CNT with a higher aspect ratio of the tube can have a larger field enhancement, and thus have a lower *E*_{to} and a higher emission current.¹² Because the CNT tube arrays were grown out of the AAO nanopore channels, the three samples have a similar tube diameter about 75 nm. The average tube lengths protruding out of the AAO surface are estimated to be 1230 nm, 1110 nm, and 237 nm for CNTs grown with CH₄ concentrations of 9%, 50%, and 91%, respectively. Thus the tube aspect ratios of the three CNT samples are 26.3, 24.7, and 13.0, respectively, when the height of the CNT portion imbedded in the AAO template, which is about 740 nm thick, is taken into account. According to the *J*–*E* curve shown in Fig. 2, at applied fields below 6 V/μm, the emission current density difference between the two denser CNT samples is more than three orders. This is far more than expected for such a small difference in the aspect ratio between the two samples. The large differences in the *E*_{to} and the emission current density between the two samples can thus be attributed to the field-screening effect. Moreover, compared with the CNTs grown with 91% CH₄, the film with 9% CH₄ shows inferior field-

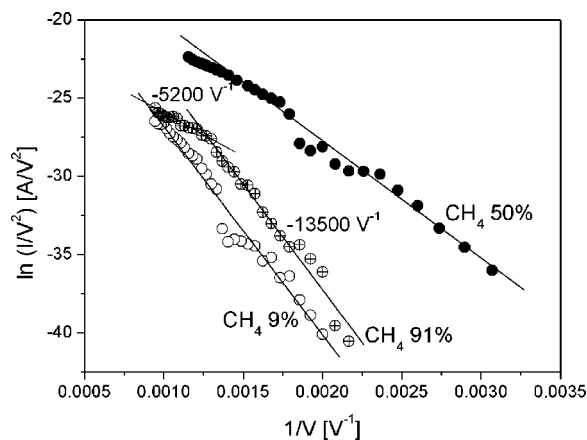


FIG. 3. Corresponding F–N plots of data shown in Fig. 2. The slopes of the F–N plot for the CNTs grown at 91% CH_4 are also indicated in the figure.

emission characteristic in the low field regime. Because the film of the highest tube density has a higher aspect ratio, it would be expected to have better field emission characteristic if the field-screening effect were insignificant. Therefore the highest E_{10} and lowest emission current density of the CNT film deposited with 9% CH_4 suggests that the field-screening effect plays a significant role on the field emission property. On the other hand, although the higher tube aspect ratio of the CNT film deposited with 50% CH_4 may improve the field emission property as compared with the CNTs grown with 91% CH_4 , the former has worse field-screening effect than the latter due to the higher tube density. We believe that the *a*-C deposit on the CNT tip is likely a major factor deteriorating the field emission characteristic of the CNTs grown with 91% CH_4 .

The F–N plot for the J – E curve of Fig. 2 is shown in Fig. 3. For the CNTs grown with 91% CH_4 , the F–N plot clearly exhibits two linear segments with a slope of about -13500 V^{-1} in the low field regime and a slope of about -5200 V^{-1} in the high field regime. The other two CNT samples do not show such an obvious slope break although they also have a nonlinear feature in the F–N plots. Nonlinearity of F–N plots for CNTs has been widely reported, and, in general, is ascribed to space charge effect¹³ and/or energy barrier modification by an dielectric overlayer deposited on the CNTs during CNT growth.^{14,15} Breakdown of the dielectric overlayer¹⁶ are also proposed to be responsible for the nonlinear behavior. However, the breakdown of the dielectric overlayer is excluded since the field emission result is reproducible. If the CNT tip is heavily coated by the *a*-C deposit, the effective local work function and conductivity of the emitter can be significantly modified, resulting in a marked deviation from the normal F–N plot. As discussed previously, during the CNT growth, *a*-C is deposited on the AAO surface and, possibly, the CNTs as well, and the amount of *a*-C deposit increases with increasing the CH_4 concentration in the gas mixture. For a very thin *a*-C overlayer, electrons emitted from the CNT can easily tunnel through the thin *a*-C dielectric layer under a moderate electric field. The work function modification on the emitter tip might just slightly alter the emission current and thus the E_{10} . But as the dielectric overlayer becomes thicker, the width of the energy bar-

rier becomes wider, and thus electrons tunneling through the dielectric layer become difficult. A higher electric field is required to decrease the effective barrier height and narrow the barrier width so that electron tunneling and thus field emission can become thriving. Moreover, it has been reported that resistance present in the field emitter structure can lead to field emission degradation.¹⁷ If the emitter resistance or the emission current is large, a potential drop through the emitter will occur, lowering the local field at the emission site. This can cause deviation of the field emission from the normal F–N characteristic in the high emission current regime. Because significant *a*-C deposit is present on the CNT film grown with 91% CH_4 , the potential drop occurring through the dielectric overlayer at the emission site as field emission electrons leave CNT tips will be larger than that of the other two samples. This is probably an important reason why the CNT sample grown with 91% CH_4 has the F–N plot remarkably different from that of the other two samples, which have much less *a*-C deposit during the CNT growth.

In summary, the tube density and length of CNTs grown from the AAO nanopores vary with the CH_4/H_2 feed ratio. A high CH_4 concentration leads to the heavy deposition of an *a*-C deposit on the AAO surface. Although the *a*-C can effectively decrease the CNT density on the AAO template, thereby decreasing the field-screening effect and increasing the field enhancement, it notably deteriorates the electron field emission property of the CNTs. The nonlinearity of the F–N plot of the CNTs is ascribed to the deposition of the *a*-C overlayer on the CNT tip. The CNTs grown at 50% CH_4 show the best field emission property.

This work was supported partly by the National Science Council of Taiwan, under Contract Nos. NSC92-2210-M-009-001 and NSC93-2120-M-009-007.

¹Yahachi Saito and Sashiro Uemura, *Carbon* **38**, 169 (2000).

²J. Li, C. Papadopoulos, J. M. Xu, and M. Moskovits, *Appl. Phys. Lett.* **75**, 367 (1999).

³Y. C. Sui, D. R. Acosta, J. A. González-León, A. Bermúdez, J. Feuchtwanger, B. Z. Cui, J. O. Flores, and J. M. Saniger, *J. Phys. Chem. B* **105**, 1523 (2001).

⁴Soo-Hwan Jeong, Ok-Joo Lee, and Kun-Hong Lee, *Chem. Mater.* **14**, 1859 (2002).

⁵L. Nilsson, O. Groening, C. Emmenegger, O. Kuettel, E. Schaller, and L. Schlapbach, *Appl. Phys. Lett.* **76**, 2071 (2000).

⁶H. Masuda and K. Fukuda, *Science* **268**, 1466 (1995).

⁷R. T. K. Baker, *Carbon* **27**, 315 (1989).

⁸Soo-Hwan Jeong, Ok-Joo Lee, Kun-Hong Lee, Sang-Ho Oh, and Chan-Gyung Park, *Chem. Mater.* **14**, 4003 (2002).

⁹K. B. K. Teo, M. Chhowalla, G. A. J. Amaratinga, W. I. Milne, G. Pirio, P. Legagneux, F. Wyczisk, J. Olivier, and D. Pribat, *J. Vac. Sci. Technol. B* **20**, 116 (2002).

¹⁰Olivier M. Küttel, Oliver Groening, Christoph Emmenegger, and Louis Schlapbach, *Appl. Phys. Lett.* **73**, 2113 (1998).

¹¹I. Brodie and P. Schwoebel, *Proc. IEEE* **82**, 1006 (1994).

¹²C. J. Edgcombe and U. Valdre, *Solid-State Electron.* **45**, 857 (2001).

¹³N. S. Xu, S. Z. Deng, and J. Chen, *Ultramicroscopy* **95**, 19 (2003).

¹⁴Hiroyoshi Tanaka, Seiji Akita, Lujun Pan, and Yoshikazu Nakayama, *Jpn. J. Appl. Phys., Part 1* **43**, 864 (2004).

¹⁵H. Gao, C. Mu, F. Wang, D. S. Xu, K. Wu, and Y. C. Xie, *J. Appl. Phys.* **93**, 5602 (2003).

¹⁶P. G. Collins and A. Zettl, *Phys. Rev. B* **55**, 9391 (1997).

¹⁷O. Groning, O. M. Küttel, P. Groning, and L. Schlapbach, *J. Vac. Sci. Technol. B* **17**, 1970 (1999).